Cover Page

Universiteit Leiden

Leiden University Repository

The handle http://hdl.handle.net/1887/19776 holds various files of this Leiden University dissertation.

Author: Runtuwene, Vincent Jimmy
Title: Functional characterization of protein-tyrosine phosphatases in zebrafish development using image analysis
Date: 2012-09-12

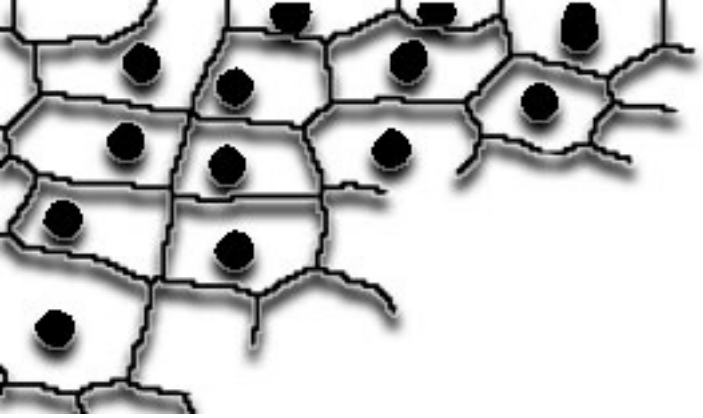

5

5

Cell Outliner and Cell Roses: New Tools for Automated Cell Membrane Detection and Determination of Cell Polarity

Vincent Runtuwene and Jeroen den Hertog

Abstract

Quantitative analysis and clear presentation of the data is essential for modern day biology. For instance, phenotypic analysis of convergence and extension cell movement defects involves quantitative analysis of defects in cell polarization. Cell polarization underlies convergence and extension cell movements during gastrulation, which are the driving forces behind the formation of the three germ layers and the shaping of an anterior-posterior axis from a radially symmetrical blastula stage embryo. The annotation of the cell membranes required for analysis of cell polarization is usually carried out manually, making it time consuming, tedious and subjective. Here we describe tools that we developed that enable ratiometric analysis of cell shape and direction, "Cell Outliner" and an integrated method to present these data, "Cell Roses". Cell Outliner is an automated image processing-based algorithm to detect membranes in 2D images. It performs a series of conversions of the original images, including adaptive thresholding, resulting in accurate detection and representation of fluorescent cell membranes. The algorithm is fast, objective and accurate. Cell Roses is a graphical application to depict cell shape and orientation in the same graph. As proof-of-principle, we successfully applied these new tools in the analysis of the presomitic mesoderm of a known zebrafish convergence and extension mutant.

The analysis of cell shape and orientation is widely used to assess differences in many biological processes. We emphasize that these tools are by no means restricted to analysis of gastrulation cell movements in zebrafish. To underline this, we have used these tools to model cell images from four distinct sources. We have made Cell Outliner and Cell Roses available for quantitative analysis of cell shape and direction in any 2D image.

Introduction

Cell polarization and directed cell migration are at the basis of many processes in embryonic development. For proper description of cell polarization and direction, and to be able to quantitatively determine differences in these parameters between (groups of) embryos, it is imperative to accurately measure the cell shape and direction of cells. For instance, the evolutionary conserved convergence and extension (CE) cell movements during zebrafish gastrulation are highly characteristic and remodel the evidently undiversified zebrafish blastula stage embryo into a complex elongated structure consisting of three germ layers, and clearly defined structures along the anterior posterior axis [1]. Medio-lateral cell elongation and orientation underlie these morphogenetic movements in the dorsal mesodermal and ectodermal cells [2,3,4,5,6]. Phenotypical analysis of cellular layers in CE phenotypes relies on quantitative information of individual cells within a tissue, collected from microscopic images. The detection of cell boundaries in these images is often carried out manually [2,5,7], which is labor intensive, error-prone, time-consuming and subjective. Therefore, great potential lies in automated image analysis for enhancing reproducibility, accuracy, speed and objectivity. Recently, efforts have been made to develop automated microscopy image analysis techniques focused on detection of cellular features [8,9]. While a growing number of studies report algorithms for localization, detection, and analysis of nuclei, only a few have been described for cell membranes. The reason for this lies in the inherent difference between detection of fluorescent nuclear markers compared to cell membrane markers. Fluorescent nuclear markers mark a volume within the cell. As a consequence, a signal from a three-dimensional source is generated upon laser-excitation which can be sufficiently sampled to create a relatively well-defined representation of the nucleus in the resulting image, making nuclei relatively straightforward to detect [10]. The sheet-like structure of the cell membrane is much thinner than the diameter of the nucleus. In fact, the cell membrane is thinner than the point spread function which marks the resolution of a standard scanning point confocal microscope[11]. Detection of a fluorescently tagged membrane can only result from sufficient sampling and interpolation of emitted light from neighboring markers, thus creating a more diffuse boundary in the confocal images. Consequently, the pixel intensities generated by the membrane signal fluctuate. As a result, the fluorescence intensity of the cell membrane that is detected is subject to the proximity of membrane junctions, adjacent cell membranes, and marker aggregations [10]. These characteristics make the detection of fluorescent membranes more cumbersome.

The problem of automated segmentation of cell membranes such as depicted in Fig. 1A has been addressed before. An anisotropic plate diffusion fil-

tering method has been proposed, which detects and enhances cell membranes using an image Hessian's eigensystem, followed by a diffusion tensor, applicable to confocal 3-D data sets [10]. Another method applies a series of artificial neural networks for the detection of neuronal membranes in 2D for electron microscopy images [12]. The use of both abovementioned methods requires intensive computation power, knowledge of computation, and in the case of artificial neural networks specialized hardware, making their use currently unfeasible for most standard biological research labs. The use of simple morphological operators has been described to detect and model cell geometries in early sea urchin embryos, which have the advantage of being less computationally intensive to execute [13]. The method takes advantage of the more conveniently detectable cell nuclei and extrapolates the location of the cell membrane by applying voronoi tessellation on the nuclear center positions [13]. This method performs accurately when applied to relatively circular cells in which the nucleus is, in fact, in the center of the cell cytoplasm (see yellow arrowhead in Fig. 1B). However, wildtype zebrafish dorsal mesodermal and ectodermal cells are elongated during CE movements and their nucleus is more often than not biased from the center of the cell cytoplasm. Applying this method on these cells results in a model in which cell elongation is underestimated, modeling elongated cells closer to a circular shape (see red arrowheads in Fig. 1B). The presence of cells in which the nucleus does not reside in the center of the cytoplasm causes an inaccurate shift in the estimated position of the cell membrane in the direction of the nucleus (see blue arrowhead in Fig. 1B).

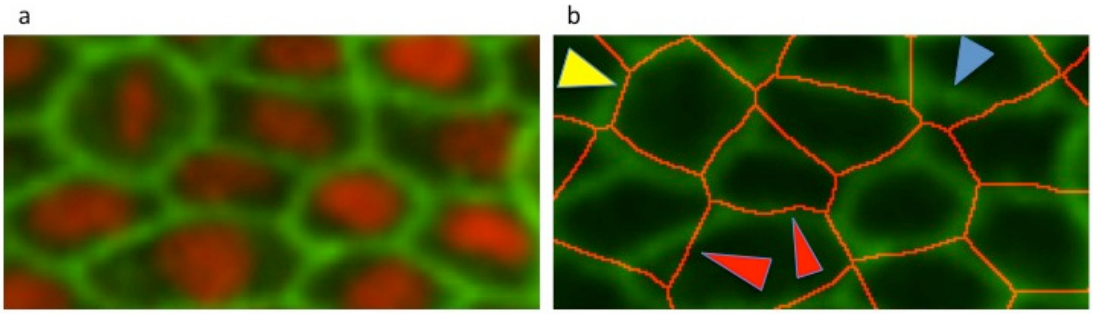

Figure 1: Application of voronoi tessalation membrane modelling method based on detection of nuclear center positions.
(A) Raw confocal image of presomitic mesoderm of an embryo micro-injected with 20 pg of YFP-CAAX mRNA, a membrane marker, and 20 pg of H2B-mCherry mRNA, a nuclear marker. (B) Voronoi diagram based on the nuclear fluorescence superimposed onto the raw membrane channel. The yellow arrowhead indicates a circular cell shape that was accurately segmented. The red arrowheads indicate 2 cells of which the modeled membranes result in an underestimation of the cell polarization. The blue arrowhead points at a cell in which the cell nucleus is offset from the center of the cytosol resulting in an inaccurate modeling of the membrane position.

Here, we report a new method for analyzing cell polarity during zebrafish CE movements. We created a new Cell Outliner algorithm as a plugin for ImageJ for automated detection and modeling of cell membranes, which employs image filtering and morphological operators in images acquired using a standard scanning point confocal microscope. The process is fast and accurate and utilizes voronoi tessellation based on the detection of cell cytoplasms rather than cell nuclei. Additionally, we employed Cell Roses to represent data on cell elongation and orientation in the same graph. This composite graph shows the correlation between cell elongation and orientation in a single view. We successfully analyzed the presomitic mesoderm in zebrafish mutants, that have a well-studied defect in CE movements, to validate the use of Cell Outliner and Cell Roses as a tool for phenotypical analysis. This tool can be adapted to any 2-D image of cells in which the cell membrane is highlighted to assess cell shape and direction in an automated manner and we have analyzed images from four distinct origins.

Materials and methods

Zebrafish maintenance, in vitro transcription of mRNA, and injection

Zebrafish were kept and the embryos were staged as described before [14]. Only wild type embryos up to 3 dpf were used for these experiments, which does not require approval of the animal experiments committee according to national and European law. Using the mMessage mMachine kit (Ambion), we synthesized 5'-capped sense mRNA encoding membrane-localized citrine (a YFP variant with a C-terminal fusion of the Ras membrane localization sequence [CAAX]) (kindly provided by Jeroen Bussman of the Hubrecht Institute) or memRFP (kindly provided by Jeroen Bakkers of the Hubrecht Institute). To achieve ubiquitous fluorescent membrane labeling, the embryos were injected at the one cell stage with 20 pg of YFP-CAAX mRNA or 30 pg of memRFP mRNA.

Confocal microscopy and positioning

To visualize the cell shape in the presomitic mesoderm, live embryos were mounted in 0.75% soft agarose at the dorsal side in glass bottomed petri dishes. Using an SP2 Leica Confocal microscope the presomitic mesoderm was imaged using a 40 X oil objective. 2-D images 512 X 512 were acquired during the 2 to 3 somite stage 100 µm posterior to the developing somites in the paraxial mesoderm, lateral to the notochord. Alternatively, the epiblast was imaged at 70% epiboly stage. All images analyzed by Cell Outliner were digitally enlarged to make the surface occupied by one cell approximately 2000 pixels, which is the optimal size for Cell Outliner.

Mice and immunostainings

All mice were in the C57BI6j/CBA mixed background and were housed according to national and european law, under the licenses required in the Netherlands. Experiments were carried out under Hubrecht Institute license number HI10.01.05. Embryos were dissected and fixed according to [15]. Two distinct monoclonal rat E-cadherin antibodies (Uvomorulin/E-Cadherin from Sigma and ECCD-2 from Millipore) were used as primary antibodies for detection of the cell shapes both in 1:250 dilution. Appropriate secondary antibodies were obtained from Jackson Immunoresearch and used in 1:500 dilution. Before incubation with primary antibodies, embryos were treated with 0,1% Triton X-100 for 10-15 minutes and blocked in 1% BSA solution for 5 hours at room temperature. Incubation with primary antibodies was carried out for three days followed by 8 washes (30 minutes each, at 4°C) and overnight for secondary antibodies followed by washes. Embryos were analyzed by confocal laser scanning microscope.

Results

Cell Outliner: Automated segmentation workflow for cell membrane recognition

In order to quantitatively analyze the polarization properties of the cells making up the presomitic mesoderm it is necessary to acquire information of a large number of cells. Manual analysis is labor-intensive, error-prone and subjective. Quantitative analysis performed by mathematical algorithms is faster, more accurate and objective. However, the bottleneck in this approach lies in detection, i.e. segmentation, of the cell shape. The problem is caused by fluctuation in the intensity of the detected fluorescent signal due to mechanical noise inherent to the confocal technique and biological fluctuation, which includes background fluorescence, non-uniform distribution of marker, and fluctuations in signal due to the proximity to membrane junctions, adjacent cell membranes, and marker aggregations.

Cell Outliner was designed to compensate for intensity fluctuations, which often occur in biological samples, facilitating automatic detection of fluorescently marked cell membranes. The algorithm was optimized for images of cell populations closely compacted together marked by YFP-CAAX. More than 20 sample pictures of presomitic mesoderm of different embryos, each constituting between 40 and 60 cells were used to optimize the workflow of the algorithm. After segmentation the morphological information can be extracted.

The most important source of mechanical noise is shot noise, which can

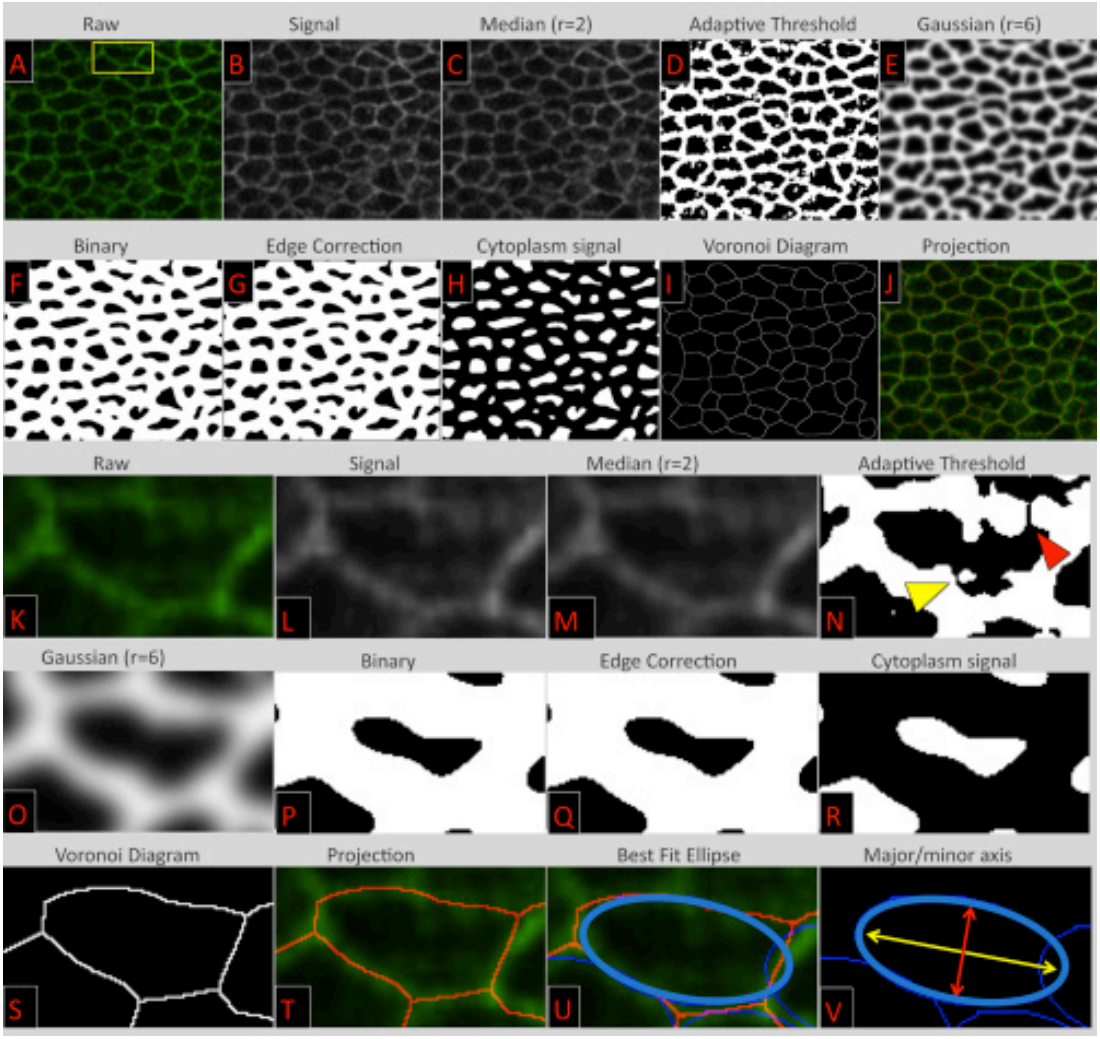

Figure 2: Workflow of the Cell Outliner Algorithm for detection and subsequent measurement of cell polarization.

Embryos were injected with 20 pg of YFP-CAAX mRNA and the presomitic mesoderm was imaged in late gastrulation stage. (A-J), Raw image and result of the Cell Outliner algorithm of a representative image of the presomitic mesoderm. (A), a raw confocal image in 8-bit colour version. (B), the signal of the YFP converted to 8-bit grayscale. (C), a median blur operation (radius=2 pixels) reduces shot noise, while preserving the edges of structures. (D), application of an adaptive thresholding procedure results in detection of the area of the cell membranes. (E), artefacts generated by the thresholding procedure are reduced greatly by applying a Gaussian blur (radius=6). (F), Binarization, using a threshold of gray value 60. (G), an Edge Correction step is applied, which converts all edge pixels to background, which is necessary for the detection of edge objects later in the procedure. (H), inversion of the signal from (G) generates an image, wherein the foreground objects represent cytosolic signals. (I), these cytosolic signals are now used to perform Voronoi tessalation, generating a Voronoi diagram, i.e. the modeled membranes. (J), the projection of the modelled membranes onto the raw confocal image. (K-T), an enlarged section of the image in (A, yellow box). N, the red arrowhead indicates a site in the thresholded image, where an abrupt change in intensity in the raw image resulted in a discontinuity in the detected membrane signal. The yellow arrowhead indicates the location of a round segmented object, caused by the presence

of a fluorescent vesicular structure present in the cytosol. (O), both these objects are eliminated by a Guassian Blur (radius=6) and subsequent binarization (P), edge correction (Q), and Voronoi tessalation (S), based on the cytoplasmic signals (R), generate an accurate model of the cell membranes. (U), projection of the best fit ellipses, in blue, onto the projection (T). (V), representation of the major (yellow) and minor (red) axis of the best fit ellipse which were used to calculate the cell elongation (aspect ratio of the length of major and minor axes) and cell orientation (the angle of the major axis of the ellipse relative to the medio-lateral direction, which is in all these images the horizontal axis).

be minimized, although its presence is inherently linked to the physical principle used by confocal microscopes. It results from the statistical variation in the number of detected photons, which can be described as a Poisson distribution [16]. As an initial step for segmentation a **median filter** with radius of 2 pixels was implemented as it was found to reduce noise greatly without affecting borders (Fig. 2A-C).

Given the common occurrence of intensity gradients in confocal images, global thresholding techniques often give poor results in separating foreground pixels (cell membranes) from the background (cytosol). Global thresholding uses a fixed threshold for all pixels in the image. It therefore works only if the intensity histogram of the input image contains neatly separated peaks, corresponding to the objects of interest. Hence, it cannot deal with images containing a strong intensity gradient. **Adaptive thresholding** (Fig. 3) is a more sophisticated technique, which selects an individual threshold for each pixel based on the range of intensity values in its local neighborhood, rather than the entire image. This allows for thresholding of an image with an intensity gradient [17]. While complex formulas have been developed to determine these local thresholds [18,19,20], we found that implementing a threshold value based on the median of the intensity

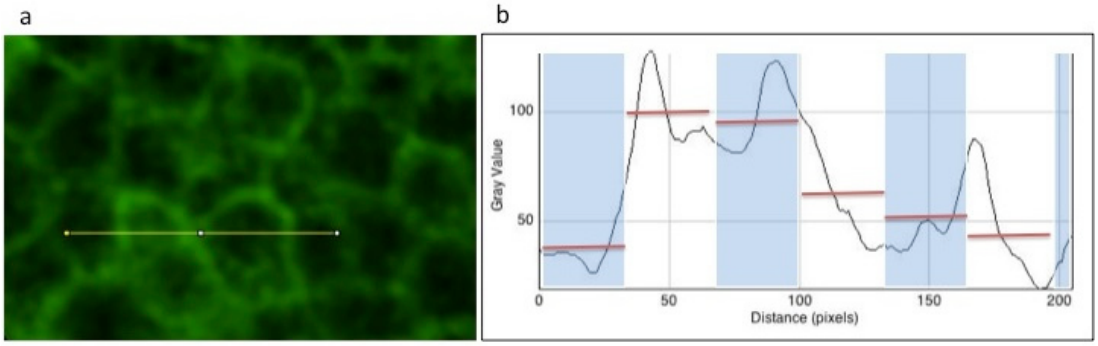

Figure 3: Adaptive Thresholding.
(A), Raw confocal image of cell membranes of an embryo injected with 20 pg of YFP-CAAX mRNA. (B), a profile plot along the region marked by the yellow line in (A). The peaks in the profile plot clearly show the regions of high membrane intensity compared to a lower cytosolic signal in between. The profile plot is subdivided in different regions, 30 pixels wide, marked by the alternating white and blue areas. Within each of these areas a separate threshold is calculated based on the median gray value of the area, which will be used for discerning the membrane signal from the local background.

of the pixels in the immediate surroundings gave the best results. A local environment of 30 X 30 pixel area around the analyzed pixel was found to be optimal (Fig. 2D).

While this method proved to be highly efficient in separating the membrane signal, two sources of error needed to be minimized. First, fluorescent vesicular structures within the cytosol occasionally create round, segmented objects (yellow arrowhead in Fig. 2N). Presence of these structures is unavoidable since these vesicles are part of the endomembrane system, which is used to traffic CAAX-tagged proteins to the plasma membrane [21]. Second, abrupt changes in membrane intensity which often occur in biological samples, can cause sites where the membrane is not detected (red arrowhead in Fig. 2N). We found a **Gaussian filter** (Fig. 2E) with a radius of six pixels followed by a **binarization,** which applied a global threshold of gray value 60 to be highly efficient in minimizing these sources of error (Fig. 2F).

The resulting image was further processed by an **edge correction** converting all pixels at the edge of the image to background (Fig. 2G). **Inversion** of this image resulted in a segmented image in which the edge of the image and the cytoplasms are foreground objects (Fig. 2H). The edge correction is needed to include cells of which the membrane is close to the edge of the image in the analysis. The reason for this lies in the next processing step: Generation of a **Voronoi diagram**. This divides an image into regions by drawing points at coordinates which are equidistant from the closest surrounding objects [22]. In other words, it subdivides the binary image into regions such that the Voronoi region of an object is the cluster of points (surface) located closest to this object. This operation is called Voronoi tessalation. By making the edge particles as well as the cytoplasms foreground, the cytoplasms close to the edge, which are in full view within the image (i.e. the ones from cells of which the plasmamembrane is close to the edge of the image), are now also included in the analysis instead of being discarded as edge objects (Fig. 2I). The Voronoi diagram is used as a binary model of the cell membranes (Fig. 2J). Close-ups of the modeling process showing a single cell are depicted in Fig. 2K-T. From the images in Fig. 2 it is apparent that the cell membranes are accurately modelled by Cell Outliner.

Efficient segmentation of membranes

To determine the efficiency of Cell Outliner for membrane segmentation, the generated membrane models were verified by manual comparison to the raw confocal images. We used samples acquired from the presomitic mesoderm of 10 embryos and all images were analyzed automatically by Cell Outliner. The program creates a second image in which a model of the membranes is generated from the raw data, and a third image in which the detected cells are numbered

and superimposed on the original raw image. In order to validate the method used by Cell Outliner, the generated objects were verified one by one by comparison of the detected/generated cell membranes in the model to their complement in the raw images.

In total 661 cells of YFP-CAAX mRNA injected embryos were analyzed and validated. Since Cell Outliner is based on the indirect detection of cytosols, a false positive is defined as a single cytosol that has been detected as multiple cytosols. A false negative is defined as an undetected cytosol. Cell Outliner showed very high efficiency: 96,89 % of the cytosols was detected correctly. The error range consisted of 2.69 % false positives and 3.10 % false negatives. The main source of false positives are rows of small, fluorescent, vesicular structures which occur occasionally within the cytosol and high intensity cytosolic signals which result from cell membranes lying in and parallel to the confocal plane. False negatives occur when the visible cytosol is very narrow, i.e. only a small part of the cytosol of the cell was visible in the confocal plane while the bulk of the cell resided either closer to the surface or deeper within the tissue.

Cell Outliner was initially designed and optimized to detect YFP-CAAX in living zebrafish embryos. However, it was highly likely that it could also be applied to detect fluorescent cell membranes in different samples. To test this, we determined its efficiency when using data from live imaging of gastrula stage zebrafish embryos injected with mRNA of memRFP, a chimeric protein containing the 10 N-terminal amino acids of GAP43 fused to N-terminus of RFP. Moreover, we used images of lateral mesoderm from fixed 4-somite stage mouse embryos that were labeled with 2 different monoclonal rat antibodies for E-Cadherin, Uvomorulin/E-Cadherin antibody or ECCD-2 (Fig. 4). Cell Outliner was shown to have a very high efficiency for all markers and cell types (> 95 %) with a low incidence of both false positives (< 2,69 %) and negatives (< 4,06 %). Cell Outliner was able to correctly identify objects in images with intensity gradients and images with low intensity were also processed with high efficiency when the membranes within the images did not appear to be interrupted. Images with low intensity in which the cells were poorly defined were not processed well and should be discarded. Cell Outliner functions consistently as it always generates the same model for a given sample. Given the objectivity and consistency of this method, multiple samples can be analyzed and compared to eachother directly. These results show that Cell Outliner is a broadly applicable, highly efficient, and consistent method to model cell membranes.

	Sample	Detected cytosols	Real total	False positives	False negatives	Efficiency
YFP- CAAX	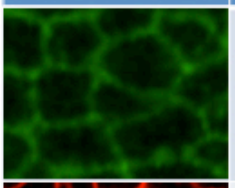	625	645	2,69 %	3,10 %	96,89 %
memRFP	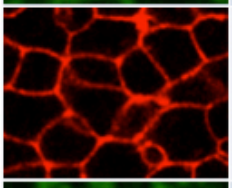	713	738	0,70 %	4,06 %	95,93 %
E-Cad	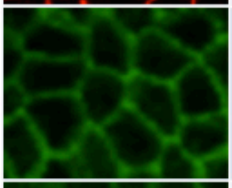	669	682	1,04 %	1,90 %	97,06 %
ECCD-2	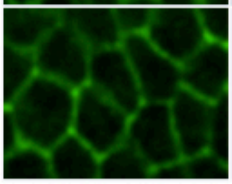	1045	1042	0,19 %	0,47 %	99,52 %

Figure 4: Cell Outliner efficiently detects cell membranes in distinct images.
Zebrafish were injected with 20 pg of YFP-CAAX mRNA and were imaged at the 2-3 somite stage or 30 pg of membrane-RFP mRNA (memRFP) and were imaged at 70% epiboly. Mice were fixed at 4 somite stage and labeled with one of 2 monoclonal anti E-cadherin rat antibodies; Uvomorulin/E-Cadherin or ECCD-2. Detection of both antibodies was done with a FITC labeled secondary antibody. Imaging was performed, focusing on mouse lateral mesoderm and zebrafish presomitic mesoderm. Confocal images were collected and analyzed by Cell Outliner, followed by manual comparison of the segment of cell membranes. A false positive is defined as a single cytosol, which is detected as (divided in) multiple cytosols. A false negative is defined as an undetected cytosol. Data from at least two independent experiments was analyzed and is presented here.

Using ImageJ, the cell shapes that were determined by Cell Outliner were analyzed by determining a best fit ellipse onto the segmented cell shapes (Fig. 2U). The length of the major and minor axis of these best fit ellipses were determined to calculate the elongation of cells, defined as the ratio of the length of major and minor axis. Additionally, the orientation of the major axis of the cells was determined as the angle this axis makes towards the medio-lateral direction (Fig. 2V). Data describing cell elongation and orientation in developing embryos is conventionally presented on separate plots [5,6,23]. Presenting these values on separate diagrams might obscure potentially valuable information regarding their correlation. Using the principle of a wind rose [24], both elongation and orientation are presented on a Cell Rose. This type of plot might reveal differences

in the correlation between cell orientation and elongation when analyzing phenotypes. To this end, we adjusted a windrose-plugin (http://www.mathworks.com) for matlab to generate Cell Roses representing both the distribution of polarization directions and intensities (here defined as aspect ratio of the best fit ellipse to the cell shape) in a colour coded radial histogram. Measurements of the direction of orientation were grouped into 10° bins and plotted as a radial histogram. Within this histogram, the area of each sector is proportional to its relative frequency (radius proportional to the square root of frequency). The length to width ratios of the best fit ellipses are calculated using Microsoft Excel and grouped into 0.2 unit bins. Each sector of the radial histogram is subdivided into smaller colour coded zones. The area of each colour coded zone is proportional to the relative frequency of elongation values within this sector. The colour code is indicated in the legend of Fig. 5. Statistical analysis of the length to width ratio was done by the student t-test assuming unequal variances. Statistical analysis of the cell orientation data was performed using Watson's U^2 square tests for significance in Matlab.

Cell Outliner and Cell Roses can be used to analyze cell polarization defects

In order to test the value of Cell Outliner and Cell Roses in the determination of cell polarization defects we analyzed wildtype and mutant embryos, with a known CE defect. *Ptpra* encodes a receptor like protein-tyrosine phosphatase which has an essential role in CE movements during gastrulation [23]. *Ptpra*-/- mutant zebrafish embryos have defects in medio-lateral elongation and orientation of mesendodermal cells. Heterozygous *ptpra*+/- fish were incrossed and the presomitic mesoderm of the embryos was imaged at late gastrulation. Subsequently, the images were analyzed using Cell Outliner and Cell Roses. We consistently found a significant loss of medio-lateral elongation and a more randomly distributed cell orientation for homozygous *ptpra*-/- mutants compared to wildtype siblings (Fig. 5), consistent with cell polarization defects in the mutants. The embryos were sequenced following imaging in order to determine their genotype. In three independent experiments a clear defect in cell polarization and orientation in the medio-lateral direction was apparent, albeit some variation was evident from experiment to experiment (Fig. 5). Yet, there was no significant difference among the wildtype samples from three independent experiments following analysis using the student t-test with unequal variances for cell elongation and the Watson U^2 test for orientation. The colour code of the Cell Roses showed that the low percentage of wildtype cells of which the orientation deviates strongly from the medio-lateral direction did not show a strong elongation (Fig.5). This is caused in part by mitotic cells, which adopt a more spherical shape and display no strong preferential orientation. Taken together, these data show that Cell Outliner and Cell Roses are powerful tools to analyze cell polarization defects with respect to elongation and direction.

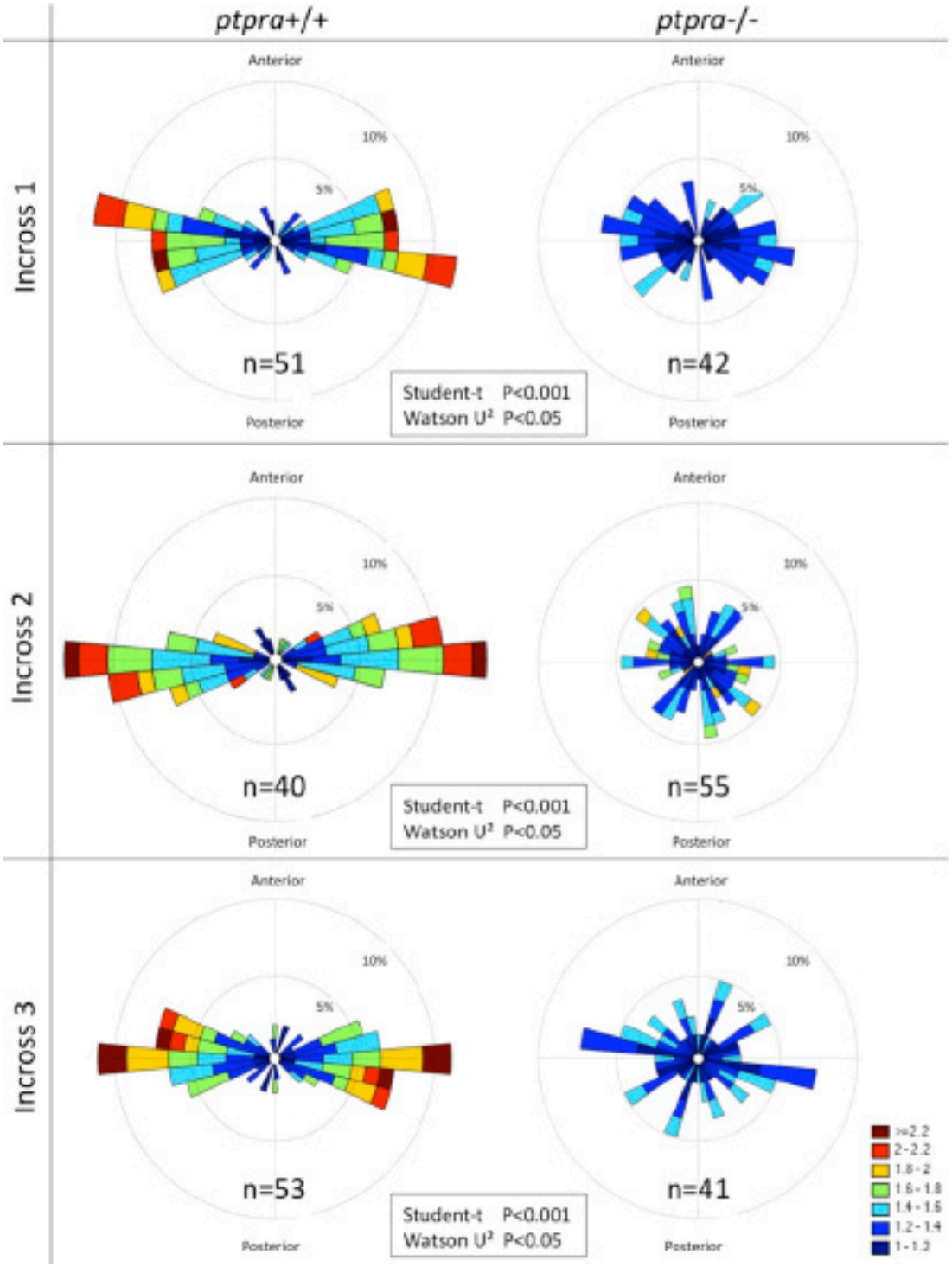
ptpra+/+
ptpra-/-
Incross 1
Incross 2
Incross 3
Anterior
Posterior
10%
5%
n=51
n=42
n=40
n=55
n=53
n=41
Student-t P<0.001
Watson U² P<0.05
>=2.2
2-2.2
1.8-2
1.6-1.8
1.4-1.6
1.2-1.4
1-1.2

Figure 5: Cell Roses are effective tools to compare, analyze and determine cell polarization defects.
In 3 independent experiments heterozygous ptpra+/- fish were incrossed and their offspring was injected with 20 pg YFP-CAAX mRNA. The embryos were imaged at the 2-3 somite stage and subsequently, genotyped by sequencing. The resulting images were processed by Cell Outliner and the resulting data was plotted using Cell Roses. These graphs show the distribution of the orientations of the cells in the presomitic mesoderm in radial histograms. Two circles on the graphs represent the 5% (inner circle) and 10% (outer circle) population fraction markers for the radial histogram. Within the bars of the histogram, a second subdivision is shown, indicating the frequencies (by surface area) and intensity of elongation (aspect ratio is indicated in colour code as indicated in the legend, bottom right) of cells within that particular population. Student-t statistics was used to compare the cell elongation values and Watson U2 statistic was used to compare the orientation data of the cells.

Discussion

Cell Outliner was designed to detect cell membranes in samples with high cell density, marked with fluorescent membrane markers, acquired through confocal imaging. It has been validated *in vivo* in zebrafish embryos for the membrane markers YFP-CAAX, in which the C-terminal CAAX-motif mediates association with the cell membrane [21], and memRFP, containing the N-terminal sequence of GAP43, which mediates association with the cell membrane [25,26]. Imaging of zebrafish embryos with ubiquitous expression of these markers yielded images of cell sheets with high density and a high fluorescence intensity signal at the cell membrane, and occasionally low intensity vesicular structures in the cytosol. Some images, used for analysis, contained fluctuation of signal intensity within a membrane segment or a global intensity gradient. The method has shown to be robust in handling gradual intensity changes and has shown to be able to compensate for small abrupt changes of intensity, producing very accurate results for these markers.

We also showed the method to be effective in fixed 4 somite stage mouse embryos labeled with 2 antibodies for E-cadherin, demonstrating a wide compatibility and applicability. Cell Outliner can in principle be used in other model organisms or any *in vivo* or *in vitro* model yielding images describing data in 2D array format in which the cell membranes are labeled. Cell Outliner may be applicable for alternative purposes as well. However, it is essential to confirm that the objects of interest are of comparable size (in pixels) to the cells it was designed to model since the numerical values used in the algorithm were optimized for this purpose.

The defining parameters for the determination of cell polarization defects are quantifications of cell elongation and medio-lateral orientation. Conventionally, these are analyzed and represented separately. In doing so, there is a potential loss of information about the correlation between the aforementioned param-

eters. By representing both on a Cell Rose, the well-studied correlation between medio-lateral elongation and orientation of the presomitic mesoderm was clear for the wildtype samples. We demonstrated the combined use of Cell Outliner and Cell Roses for analyzing the mutant phenotype of *rptpa* in the presomitic mesoderm of zebrafish embryos. The cell roses clearly showed the concomitant loss of elongation and medio-lateral orientation of the cells in the mutant.

Application and Conclusion

The necessity of determining and scoring individual cell behaviours and polarity as part of a population or tissue is not restricted to the study of gastrulation. In development alone numerous examples can be found in which polarity and tissue migration are key factors, like in angiogenesis [27] and the establishment of the highly organized structure of auditory and vestibular epithelia [28]. Collective tissue migration also underlies wound healing; the basal random individual movements of the endothelial cells are reoriented to collectively polarized migration by modular control, independent from growth factors, upon the appearance of cell free space [29]. Similar cell behaviors have also been observed in metastatic processes in mouse mammary tissue [30]. The advent of more sophisticated imaging technology, including hardware and a plethora of highly sensitive and specific fluorescent probes, allows the visualization of these biological processes in unprecedented detail. Data analysis of these huge data sets for morphological features can be greatly facilitated by the use of algorithms like Cell Outliner.

Cell Outliner is a freely available ImageJ plug-in (http://rsbweb.nih.gov/ij/plugins/), which works with ImageJ version 1.45h or higher. The application is very simple: install as an ImageJ plugin, and the application will appear in the scroll-down menu within the ImageJ program. Apply to an 8-bit image (or stack of images) representing the cell membranes: the output contains the original image, an image of the generated model, a projection of the detected objects onto the original image and a table with the data of the analyzed cells. The method eliminates the need for conventional, labor-intensive, manual annotation of the membranes and is extremely fast, objective, reliable, and reproducible. Since Cell Outliner facilitates the collection of information regarding a commonly used phenotypic parameter like cell shape, it can be applied to a wide range of phenotypes and is certainly not limited to the zebrafish or mouse model.

Cell Roses is a freely available plugin (upon request) for Matlab, which can be used to plot the output of Cell Outliner. The data generated by Cell Outliner, which is in an excel format, can be imported into Matlab and subsequently processed. This novel method of data representation not only combines the advantages of the conventional separate representation of cell elongation and medio-

lateral orientation, it also adds additional information regarding their correlation, potentially reveiling vital information.

Acknowledgements

The authors would like to thank Monika Bialecka and Jacqueline Deschamps for kindly providing the images of mouse embryos stained with the different E-cadherin antibodies and Jeroen Bakkers and Jeroen Bussman for plasmids encoding fuorescent membrane markers. This work was supported by a Marie Curie Research Training Network (PTPNET / MRTN-CT-2006-035830). The funders had no role in study design, data collection and analysis, decision to publish, or preparation of the manuscript.

References

1. Roszko I, Sawada A, Solnica-Krezel L (2009) Regulation of convergence and extension movements during vertebrate gastrulation by the Wnt/PCP pathway. Semin Cell Dev Biol 20: 986-997.

2. Myers DC, Sepich DS, Solnica-Krezel L (2002) Bmp activity gradient regulates convergent extension during zebrafish gastrulation. Dev Biol 243: 81-98.

3. Myers DC, Sepich DS, Solnica-Krezel L (2002) Convergence and extension in vertebrate gastrulae: cell movements according to or in search of identity? Trends Genet 18: 447-455.

4. Topczewski J, Sepich DS, Myers DC, Walker C, Amores A, et al. (2001) The zebrafish glypican knypek controls cell polarity during gastrulation movements of convergent extension. Dev Cell 1: 251-264.

5. Jessen JR, Topczewski J, Bingham S, Sepich DS, Marlow F, et al. (2002) Zebrafish trilobite identifies new roles for Strabismus in gastrulation and neuronal movements. Nat Cell Biol 4: 610-615.

6. Concha ML, Adams RJ (1998) Oriented cell divisions and cellular morphogenesis in the zebrafish gastrula and neurula: a time-lapse analysis. Development 125: 983-994.

7. Lin F, Sepich DS, Chen S, Topczewski J, Yin C, et al. (2005) Essential roles of G{alpha}12/13 signaling in distinct cell behaviors driving zebrafish convergence and extension gastrulation movements. J Cell Biol 169: 777-787.

8. Keller PJ, Schmidt AD, Wittbrodt J, Stelzer EH (2008) Reconstruction of zebrafish early embryonic development by scanned light sheet microscopy. Science 322: 1065-1069.

9. Megason SG (2009) In toto imaging of embryogenesis with confocal time-lapse microscopy. Methods Mol Biol 546: 317-332.

10. Mosaliganti K, Janoos F, Gelas A, Noche R, Obholzer N, et al. (2010) Anisotropic Plate Diffusion Filtering for Detection of Cell Membranes in 3d Microscopy Images. Proc IEEE Int Symp Biomed Imaging: 588-591.

11. Megason SG, Fraser SE (2007) Imaging in systems biology. Cell 130: 784-795.

12. Jurrus E, Paiva AR, Watanabe S, Anderson JR, Jones BW, et al. (2010) Detection of neuron membranes in electron microscopy images using a serial neural network architecture. Med Image Anal 14: 770-783.

13. M.A.Luengo-Oroz LD, C.Castrcfi, T.SavyK E.Faure, B.Lombardo,, P.Bourgine NPaAS (2008) Can voronoi diagram model cell geometries in early sea urchin embryogenesis? ISBI: 504-507.

14. Westerfield (1995) The zebrafish book: University of Oregon press, Eugene, Oregon.

15. Lawson KA (1999) Fate mapping the mouse embryo. Int J Dev Biol 43: 773-775.

16. Pawley JB (2006) Handbook of biological confocal microscopy.

17. Davies E (1990) Machine vision: theory, algorithms and practicalities: Academic press.

18. Bernsen J. Dynamic Thresholding of Grey-Level Images; 1986.

19. Niblack W (1986) An introduction to Digital Image Processing: Prentice-Hall.

20. Sauvola J, Pietaksinen M (2000) Adaptive Document Image Binarization. Pattern Recognition 33: 225-236.

21. Choy E, Chiu VK, Silletti J, Feoktistov M, Morimoto T, et al. (1999) Endomembrane trafficking of ras: the CAAX motif targets proteins to the ER and Golgi. Cell 98: 69-80.

22. Aurenhammer F (1991) Voronoi Diagrams - A Survey of a Fundamental Geometric Data Structure. ACM Computing Surveys 23: 345-405.

23. van Eekelen M, Runtuwene V, Overvoorde J, den Hertog J (2010) RPTPalpha and PTPepsilon signaling via Fyn/Yes and RhoA is essential for zebrafish convergence and extension cell movements during gastrulation. Dev Biol 340: 626-639.

24. Slade DH (1968) Meteorology and atomic energy: US Atomic Energy Commission. 28-30 p.

25. Greaves J, Prescott GR, Fukata Y, Fukata M, Salaun C, et al. (2009) The hydrophobic cysteine-rich domain of SNAP25 couples with downstream residues to mediate membrane interactions and recognition by DHHC palmitoyl transferases. Mol Biol Cell 20: 1845-1854.

26. Greaves J, Salaun C, Fukata Y, Fukata M, Chamberlain LH (2008) Palmitoylation and membrane interactions of the neuroprotective chaperone cysteine-string protein. J Biol Chem 283: 25014-25026.

27. Cirone P, Lin S, Griesbach HL, Zhang Y, Slusarski DC, et al. (2008) A role for planar cell polarity signaling in angiogenesis. Angiogenesis 11: 347-360.

28. Kelly M, Chen P (2007) Shaping the mammalian auditory sensory organ by the planar cell polarity pathway. Int J Dev Biol 51: 535-547.

29. Vitorino P, Meyer T (2008) Modular control of endothelial sheet migration. Genes Dev 22: 3268-3281.

30. Wyckoff JB, Wang Y, Lin EY, Li JF, Goswami S, et al. (2007) Direct visualization of macrophage-assisted tumor cell intravasation in mammary tumors. Cancer Res 67: 2649-2656.